Impact of Polyethylene Glycol as Additive on the Formation and Extraction Behavior of Ionic-Liquid Based Aqueous Two-Phase System

Mohammad Vahidnia, Gholamreza Pazuki, and Shiva Abdolrahimi
Chemical Engineering Dept., Amirkabir University of Technology (Tehran Polytechnic), Tehran, Iran

DOI 10.1002/aic.15035
Published online September 24, 2015 in Wiley Online Library (wileyonlinelibrary.com)

Developing a novel Ionic-liquid (IL) based aqueous two-phase system (ATPS) with polyethylene glycol (PEG) as adjuvant for the separation of biomolecules is studied. This original work involves addition of various concentration of PEG (2000, 4000, and 6000 gr/mol) to 1-butyl-3-methylimidazolium acetate+ potassium hydrogen phosphate ATPS to investigate their subsequent effect on phase diagrams and partitioning coefficient of α-amylase. In another innovative aspect of this work, response surface methodology (RSM) based on three-variable central composite design was employed to understand the effect of phase forming components on extraction studies of α-amylase. The addition of small amount of PEG improved the partitioning coefficient of biomolecule. The effective excluded volume theory was applied to correlate the salting-out ability. As a result, it can be stated that the proposed system can effectively be used in separation and purification studies instead of task specific ILs. © 2015 American Institute of Chemical Engineers *AIChE J*, 62: 264–274, 2016

Keywords: aqueous two-phase system, ionic liquid, partition coefficient, response surface design

Introduction

The manufacture of pure biological active substances is widely significant as the final cost is entirely related to the purification processes involved.[1] In the past decade, aqueous two-phase system (ATPS) has found its platform in purification of proteins,[2–4] heavy metal ions,[5] organic molecules,[6] and antibiotic.[7–9] ATPS is typically formed when two incompatible polymer/polymer or polymer/salt are dissolved in water.[10–12] The bulk of the two immiscible phases is mainly composed of water, thus, the ATPS creates a gentle and biocompatible media for separation of biomolecule.[1,13,14] The partitioning of the biomolecule in aqueous two phase system is beneficiated by the diverse physical and chemical properties of the phases. Low toxicity, low volatility, large water miscibility and high biodegradability of polyethylene glycol (PEG) make it a viable candidate as phase-forming component in the ATPS.[15–17] Application of polymer-salt ATPS in downstream processing is more advantageous over polymer–polymer type ATPS due to its low interfacial tension, fast phase separation rates, and low costs.[15] However, tailoring chemical nature of PEG is only achievable through changes in its molecular weight or its structural modification. On the contrary, ionic liquids (ILs) can effectively overcome these limitations.

In 2003, Rogers and coworkers[18] observed phase separation while adding inorganic salts to aqueous solutions of ILs. Ionic liquids are salts which are in liquid form at temperature below 100°C. The remarkable physical and chemical properties of ILs such as negligible vapor pressure, nonflammability, tunability, high selectivity, and a wide liquid range make their industrial application appealing.[13] Recent advances have focused on application of ILs as an alternative to polymer based ATPS.[19–24] The main advantage of IL-based over polymer-based ATPS is the possibility of controlling the phases polarities by a suitable manipulation of cation-anion combinations.[14] Moreover, hydrophilic/lipophilic balance of polymers is more limited.[25,26]

To modify the intrinsic properties of ATPS some researchers have used a promoter or adjuvants of ATPS formation. Pereira et al.[15] applied various imidazolium based ILs as adjuvants to conventional PEG/inorganic salt ATPS. They observed that the salting-in/salting-out aptitude of ILs can largely influence L-tryptophan extraction. Moreover, Almeida et al.[17] have recently shown that IL can tune the polarity of PEG-rich phase and its chemical nature can affect the extraction of phenolic acids. Many researchers have attempted in enhancement of extraction ability of ILs. The concept of task specific ILs was originally proposed by Davis, Rogers, and coworkers.[27] Liquid–liquid extraction of mercury (II) and cadmium (II) were investigated by incorporation of ion-ligating groups into imidazolium cation. Appending metal-ion ligating group to IL increased the metal ion distribution ratios by several orders of magnitude.[27,28]

In conventional methods of studying a process, one factor is varied while maintaining other factors at an unspecified constant level. These methods, apart from being time-consuming and requiring a large number of experiments, do not determine the interaction among the variables.[29,30] Statistical

Correspondence concerning this article should be addressed to G. Pazuki at ghpazuki@aut.ac.ir.

experimental design such as response surface methodology (RSM) is developed to overcome the limitations of conventional methods. RSM improves and optimizes the process and evaluates the significance of affecting parameters. Moreover, in the presence of complex interactions, it effectively studies the interactions among the variables.

To modify the characteristics of the IL-rich phase, a new approach, making use of PEG is developed. PEG with various molecular weights has been used as a promoter or adjuvant of ATPS formation. Consequently, the phase behavior of IL-K_2HPO_4 in presence of various concentration of PEG has been studied. The extraction ability of IL-K_2HPO_4 in presence of PEG is evaluated using α-amylase as model biomolecule. The effect of initial concentration of IL, K_2HPO_4, and PEG on partitioning coefficients of α-amylase has been studied using RSM based on CCD.

Materials and Methods

Materials

In this study, ATPSs were established using aqueous solution of 1-butyl-3-methylimidazolium acetate, $[C_4mim]CH_3COO$ (>99% pure, Iolitec) and potassium hydrogen phosphate, K_2HPO_4 (>99% pure, Merck). The PEGs were added to the system as additives with various molecular weights, 2000, 4000, and 6000 gr/mol and are abbreviated as PEG 2000, PEG 4000, and PEG 6000, respectively. The polymers were purchased from Merck. α-amylase as the selected enzyme for partitioning studies was provided from Merck. Moreover, the chemicals were utilized without further purification. Double distilled deionized water was applied to prepare the samples.

Experimental Procedure

Phase diagrams

In most research studies, visual detection of cloud points has been the experimental basis for evaluation of the binodal curve.[7–27] Thus, the cloud point titration method was performed at (25 ± 1)°C and atmospheric pressure to determine the phase diagrams. The binodal curves of IL-based ATPS were plotted at various fixed concentrations (0, 4, and 8 wt %) of PEG 2000, 4000, and 6000 as adjuvants. Consequently, aqueous solution of K_2HPO_4 + fixed concentration of PEG, aqueous solution of $[C_4mim]CH_3COO$+desired concentration of PEG, and aqueous solution of PEG with the same concentration were prepared.

There are two fundamental experimental procedures: (1) formation of turbid biphasic solution by drop wise addition of aqueous salt solution to ionic liquid solution; (2) detection of clear monophasic region by drop wise addition of polymer solution. Subsequent compositions of each point were evaluated by weight quantification within $\pm 10^{-4}$ g. The completion of the phase diagrams were performed by addition of ionic liquid solution to salt solution. Accordingly, the experimental binodal curves were fitted to the following three-parameter equation[31]

$$[\mathrm{IL}] = A\exp\left(B[\mathrm{salt}]^{0.5} - C[\mathrm{salt}]^3\right) \quad (1)$$

where [IL] and [salt] are mass fraction percentage of the ionic liquid and inorganic salt, respectively; and A, B, and C are fitting parameters evaluated by data regression.

Determination of tie-lines

The tie-lines of a polymer-based ATPS were originally determined by a gravimetric method proposed by Merchuk et al.[31] On the basis of this method, binodal data by Eq. 1 are coupled with mass balance relationships. Consequently, each tie-line was evaluated by application of lever-arm rule between the composition of the top phase, the bottom phase, and the overall system. Thus, solving the following system of four equations and four unknowns led to the determination of TLs compositions

$$[\mathrm{IL}]_{\mathrm{top}} = A\exp\left(B[\mathrm{salt}]_{\mathrm{top}}^{0.5} - C[\mathrm{salt}]_{\mathrm{top}}^3\right) \quad (2)$$

$$[\mathrm{IL}]_{\mathrm{bot}} = A\exp\left(B[\mathrm{salt}]_{\mathrm{bot}}^{0.5} - C[\mathrm{salt}]_{\mathrm{bot}}^3\right) \quad (3)$$

$$[\mathrm{IL}]_{\mathrm{top}} = \frac{[\mathrm{IL}]_{\mathrm{M}}}{\alpha} - \frac{1-\alpha}{\alpha}[\mathrm{IL}]_{\mathrm{bot}} \quad (4)$$

$$[\mathrm{salt}]_{\mathrm{top}} = \frac{[\mathrm{salt}]_{\mathrm{M}}}{\alpha} - \frac{1-\alpha}{\alpha}[\mathrm{salt}]_{\mathrm{bot}} \quad (5)$$

where subscripts "top," "bot.," and "M" refer to the top-phase, the bottom-phase, and the mixture, respectively. Moreover, [IL] and [salt] refer to mass fraction percentage of ionic liquid and salt. The parameter α is the ratio between the mass of the top phase and the total mass of the mixture.

Furthermore, the tie-line length (TLL) and slope of TLs (STL) can be calculated according to Eqs. 6 and7

$$\mathrm{TLL} = \sqrt{\left([\mathrm{IL}]_{\mathrm{top}} - [\mathrm{IL}]_{\mathrm{bot}}\right)^2 + \left([\mathrm{salt}]_{\mathrm{top}} - [\mathrm{salt}]_{\mathrm{bot}}\right)^2} \quad (6)$$

$$\mathrm{STL} = \frac{[\mathrm{IL}]_{\mathrm{top}} - [\mathrm{IL}]_{\mathrm{bot}}}{[\mathrm{salt}]_{\mathrm{top}} - [\mathrm{salt}]_{\mathrm{bot}}} \quad (7)$$

Design of experiments

Studying a process based on conventional methods involves changing a single factor while keeping all the other factors at constant levels. Consequently, these methods are time-consuming and require a large number of experimental runs. However, they do not give the combined effect of all the process variables.[29] As a result, limitations of the conventional methods necessitate the application of a statistical experimental design, such as RSM, which optimizes the process variables.[29,30] Consequently, the design of experiment based on RSM evaluates regression models along with the effect of process variables in the presence of complex interactions.[32,33] A well-known standard RSM design is central composite design (CCD); it was applied as the basis of this research to study the effect of process variables on partitioning of α-amylase. The design of experiments (DOE) based on CCD consists of 2^n axial runs with $2n$ full factorial runs and also n_c replicates at the center points.

The effect of different process variables on the partitioning of α-amylase in IL-K_2HPO_4 ATPS with PEG as adjuvants were studied with a central composite face centered design. In this research, the studied independent variables were (1) X_1: $[C_4mim]CH_3COO$ mass fraction percentage in the feed; (2) X_2: K_2HPO_4 mass fraction percentage in the feed; and (3) X_3: PEG concentration in the ATPS. Moreover, the partitioning coefficient of biomolecule was selected as the dependent output response variable

Table 1. Experimental Range and Levels of Independent Process Variables for α-amylase Extraction in IL-Based ATPS

	Ranges and Levels		
Independent Variables	(−1)	(0)	(+1)
$[C_4mim]CH_3COO$ (X_1)	10	12.5	15
K_2HPO_4 (wt %) (X_2)	30	32.5	35
PEG (wt %) (X_3)	0	4	8

$$K_{\alpha\text{-amylase}} = \frac{[\alpha\text{-amylase}]_{IL}}{[\alpha\text{-amylase}]_{salt}} \quad (8)$$

where $[\alpha\text{-amylase}]_{IL}$ is the concentration of α-amylase in the IL-rich phase and $[\alpha\text{-amylase}]_{salt}$ is its respective concentration in the K_2HPO_4-rich phase.

In this study 2^3 full factorial CCD for 3 variables and 2×3 axial points were used. The independent variables, X_i, were coded as x_i based on the following equation

$$x_i = \frac{(X_i - X_0)}{\partial X} \quad (9)$$

where x_i is the coded value of i th independent variable, X_i the natural value of ith independent variable, X_0 the natural value of the ith independent variable at the center point, and ∂X is the value of step change.

Table 1 demonstrates the independent variables along with their coded and uncoded values for all three systems based on the molecular weight of PEG. A mathematical relationship between the dependent response and the independent variables can be evaluated. Consequently, each set of responses was employed to develop an empirical model using a second degree polynomial equation

$$Y = b_0 + \sum_{i=1}^{n} b_i x_i + \sum_{i=1}^{n} b_{ii} x_i^2 + \sum_{i=1}^{n-1} \sum_{j=i+1}^{n} b_{ij} x_i x_j \quad (10)$$

where Y is the predicted response, b_0 the constant coefficient, b_i the linear coefficients, b_{ii} the quadratic coefficients, b_{ij} the interaction coefficients; and x_i, x_j are the coded values of independent process variables.

Table 2 shows the complete design matrix. The required IL-based ATPS with a desired amount of PEG as the additive is formulated to get the required composition in DOE table. Furthermore, a suitable amount of α-amylase was added to get the concentration of 0.4 wt %. The prepared mixtures were stirred and kept in small decanters for 24 h for complete phase separation. To eliminate the temperature effect, all samples were incubated at (25 ± 1)°C. Additionally, the same mass fraction percentages were used for tie-line determinations.

The regression and graphical analysis was performed by MINITAB 16 statistical software.

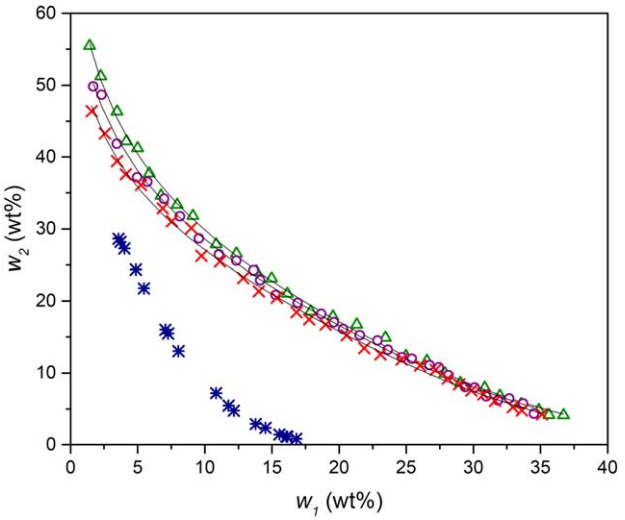

Figure 1. Evaluation of the PEG 2000 effect in the ternary phase diagrams composed of $[C_4mim]CH_3COO$ (2)+ K_2HPO_4(1)+ H_2O.

△, 0% PEG 4000; ○, 4% PEG 2000; ×, 8% PEG 2000; and ✱, PEG 2000 (2)+ K_2HPO_4 (1) (no IL). [Color figure can be viewed in the online issue, which is available at wileyonlinelibrary.com.]

Results and Discussion

Phase diagrams

Since all the biphasic systems share the same inorganic salt as well as IL, and also pressure and temperature were held constant, the comparison of the binodal data results in to the comprehension of the effect of molecular weight and concentration of PEG on ATPS formation. Figures 1–3 represent the

Table 2. CCD Design Matrix Along with Experimental and Predicted Response Values

				Partition Coefficient					
				PEG 2000		PEG 4000		PEG 6000	
Std. Order	x_1	x_2	x_3	Experimental	Predicted	Experimental	Predicted	Experimental	Predicted
1	−1	−1	−1	9.36	9.360829	9.25	9.239592	9.3	9.327697
2	1	−1	−1	14.6	14.56873	14.52	14.64239	14.62	14.4901
3	−1	1	−1	11.35	11.33363	11.41	11.56749	11.33	11.8111
4	1	1	−1	19.2	18.86253	19.13	18.54479	19.19	18.694
5	−1	−1	1	11.99	11.45013	10.77	11.32619	9.31	9.840997
6	1	−1	1	16.1	16.65803	13.99	13.79249	12.54	12.0869
7	−1	1	1	16.54	15.75593	15.95	15.78859	15.01	15.1639
8	1	1	1	22.75	23.28483	19.85	19.82939	19.11	19.1303
9	−1	0	0	13.25	14.60349	14.05	13.52413	14.12	12.96331
10	1	0	0	21.56	20.97189	17.55	18.24593	16.45	17.52771
11	0	−1	0	14.35	13.94364	13.75	13.29833	12.69	12.74731
12	0	1	0	18.12	18.24344	16.85	17.48073	17.65	17.51071
13	0	0	−1	11.32	11.83729	11.26	11.59573	11.45	11.59811
14	0	0	1	14.85	15.09309	13.45	13.28133	12.31	12.07291
15	0	0	0	16.56	16.09354	15.01	14.68587	14.01	14.19596

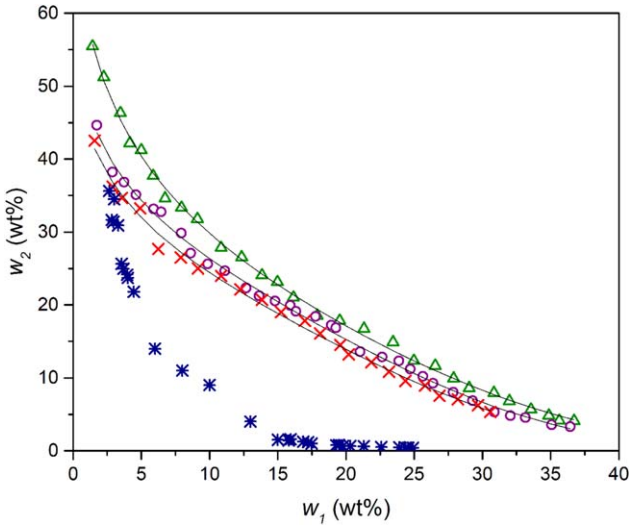

Figure 2. Evaluation of the PEG 4000 effect in the ternary phase diagrams composed of [C_4mim]-CH_3COO (2)+ K_2HPO_4 (1) + H_2O.

△, 0% PEG 4000; ○, 4% PEG 4000; ×, 8% PEG 4000; and ✳, PEG 4000 (2)+K_2HPO_4(1)(no IL). [Color figure can be viewed in the online issue, which is available at wileyonlinelibrary.com.]

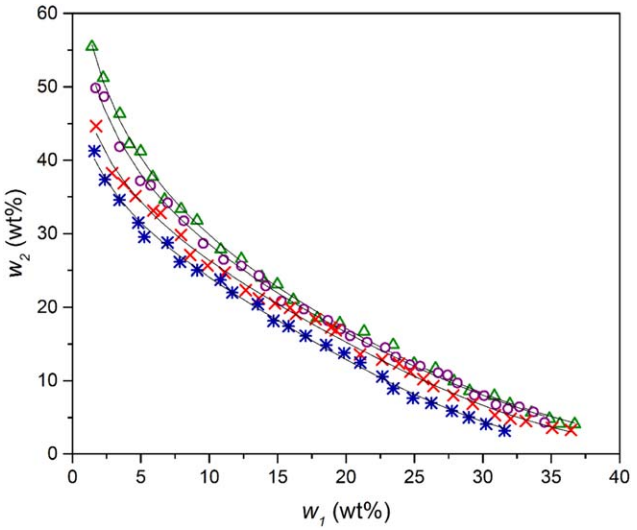

Figure 4. The evaluation of the effect PEG with various molecular weights in the ternary phase diagrams composed of [C_4mim]CH_3COO (2)+ K_2HPO_4(1)+ H_2O.

△, 0% PEG; ○, 4% PEG 2000; ×, 4% PEG 4000; and ✳, 4% PEG 6000. [Color figure can be viewed in the online issue, which is available at wileyonlinelibrary.com.]

experimental phase diagrams for [C_4mim]CH_3COO+ K_2HPO_4+H_2O+PEG 2000, 4000, or 6000, respectively. The binodal curve for the control system without PEG is also plotted in all figures to enhance the comparison. Moreover, it should be stressed out that the PEG concentration was held constant along each binodal curve.

Generally, the biphasic region is located above the saturation curve. Consequently, as the curve gets closer to the origin the biphasic area is extended and thus phase separation is promoted. The presented figures indicated that the presence of PEG reduced the phases' miscibility. These remarkable results were observed with the addition of PEG as adjuvants. Hence, ATPS formed by addition of PEG in small amount demonstrates a better phase separation in comparison with the ATPS formed only with the IL and inorganic salt. This result suggests that the mixtures of IL–PEG may be more "hydrophobic" than their pure counterparts and are more easily salted-out by K_2HPO_4. The ability of each ATPS to form two liquid phases is as follows

IL+ K_2HPO_4+ H_2O+ 8 wt % PEG > IL+ K_2HPO_4+ H_2O+ 4 wt % PEG > IL+ K_2HPO_4+ H_2O (no PEG). Therefore, an increase in the concentration of PEG from 0 to 8 wt % enhanced the degree of phase separation.

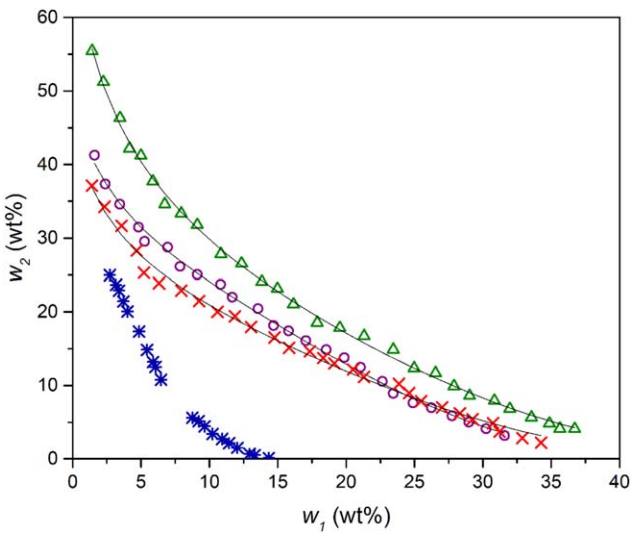

Figure 3. Evaluation of the PEG 6000 effect in the ternary phase diagrams composed of [C_4mim]-CH_3COO (2) + K_2HPO_4(1) + H_2O.

△, 0% PEG 6000; ○, 4% PEG 6000; ×, 8% PEG 6000; and ✳, PEG 6000 (2)+ K_2HPO_4(1)(no IL). [Color figure can be viewed in the online issue, which is available at wileyonlinelibrary.com.]

Figure 4 shows the impact of the molecular weight of PEG on ATPS creation. It is obvious that there is an increase in the ATPS formation ability with the increase in PEGs molecular weights. This behavior can be interpreted with the fact that higher hydrophobicity was displayed by PEGs with higher molecular weights; this means that they possess lower affinity for water, and are more easily excluded as a second liquid phase.

Nonlinear regression of the binodal data evaluated the parameters of Eq. 1, along with the corresponding correlation coefficients (Table 3). The competence of Eq. 1 in describing the experimental data was validated as the R^2-value was close to unity.

Effective excluded volume and salting-out ability

In 1993, Guan et al.[34] developed a binodal model for aqueous solution of polymers. The main concept of their theory is based on the random distribution of the molecular species in the solution, which results in a solution that is geometrically saturated of each solute in the presence of other components for each system composition along the binodal curve.[35] For evaluation of the salting-out ability of [C_4mim]CH_3COO-K_2HPO_4 with various concentration of PEGs as additive, the binodal curves were correlated based on the effective excluded volume (EEV) theory. In

Table 3. Values of Parameters (A, B, and C) of Eq. 1 for the IL-based ATPSs at $T=298.15$ K

Biphasic System	A	B	$C \times 10^5$	R^{2*}
IL+ salt+ H_2O	80.46	−0.307	2.184	0.9984
IL+ salt+ H_2O+ 4 wt % PEG 2000	73.34	−0.2914	2.279	0.998
IL+ salt+ H_2O+ 8 wt % PEG 2000	66.73	−0.2773	2.509	0.9978
IL+ salt+ H_2O+ 4 wt %PEG 4000	61.19	−0.2567	3.008	0.9967
IL+ salt+ H_2O+ 8 wt % PEG 4000	57.36	−0.2595	3.207	0.9956
IL+ salt+ H_2O+ 4 wt % PEG 6000	55.04	−0.2477	4.300	0.9974
IL+ salt+ H_2O+ 8 wt %PEG 6000	50.91	−0.2718	2.934	0.9944

*$R^2=1-\sum_1^N(Y_{\exp}-Y_{pre})^2/\sum_1^N(Y_{xp})^2$; $Y_{\exp}$ Experimental binodal data; Y_{pre} Predicted binodal data by regression.

Table 4. Values of Parameters of EEV of Salts Using Eqs. 11 or 12 for the $[C_4mim]CH_3COO$ (1) + Salt (2) + Water (3) ATPS with PEG as Additive at $T=298.15$ K

Salt	V^*_{213}	R^{2*}	sd*
No PEG	5.381	0.997	4.638
4 wt % PEG 2000	5.434	0.994	4.265
8 wt % PEG 2000	5.579	0.995	4.646
4 wt % PEG 4000	5.723	0.995	4.606
8 wt % PEG 4000	6.075	0.994	4.175
4 wt % PEG 6000	6.334	0.996	4.041
8 wt %PEG 6000	6.191	0.991	5.108

*$R^2=1-\sum_1^N(w_{\text{IL,exp}}-w_{\text{IL,pre}})^2/\sum_1^N(w_{\text{IL,exp}})^2$; $\text{sd}=(\sum_1^N(w_{\text{IL,exp}}-w_{\text{IL,pre}})^2/N)^{0.5}$; w IL, exp = Experimental IL wt % and $w_{\text{IL,pre}}$=predicted IL wt %.

the ternary system of $[C_4mim]CH_3COO$ (1) + K_2HPO_4 (2) + water (3), the excluded volume theory can be written as[32]

$$\ln\left(V^*_{213}\frac{w_2}{M_2}+f_{213}\right)+V^*_{213}\frac{w_1}{M_1}=0 \tag{11}$$

$$\ln\left(V^*_{213}\frac{w_2}{M_2}\right)+V^*_{213}\frac{w_1}{M_1}=0 \tag{12}$$

where V^*_{213}, f_{213}, M_1, and M_2 are the scaled EEV of organic salt, the volume fraction of unfilled effective available volume after tight packing of salt molecules into the network of $[C_4mim]CH_3COO$, and molecular weight of IL and inorganic salt, respectively. The EEV values obtained from the correlation of the binodal data with various concentrations and molecular weights of PEG are presented in Table 4. The EEV value is the mere indication of the compatibility of the system's components as it shows the smallest space at which each IL molecule will accept an individual salt in the presence of PEG as additive. In our work, a negligible value for f_{213} is observed. Recently, in many research studies, the EEV values and the salting-out ability of the components has been related.[36,37] Consequently, the ATPS system with larger values of EEV is composed of stronger salting-out agents. Thus, the rank order of 4 wt % PEG 6000 > 8 wt % PEG 6000 > 8 wt % PEG 4000 > 4 wt % PEG 4000 > 8 wt % PEG 2000 > 4 wt % PEG 2000> No PEG demonstrates the ability of PEG with various molecular weight and concentration to create a biphasic region.

Tie-line data and correlations

For each experimental run in DOE table the tie-line compositions were obtained. Tables 5–7 manifest the upper and lower phase compositions with their subsequent values of STL and TLL with variation of process variables. The compositions of TLs were calculated by application of gravimetric method together with solution of a system of four equations and four unknowns. As can be observed, $[C_4mim]CH_3COO$ concentration in lower phase is quite insignificant.

Moreover, the application of Othmer–Tobias[38] equation resulted in validation of tie-lines for the studied system

$$\ln\frac{100-[\text{IL}]_{\text{top}}}{[\text{IL}]_{\text{bot}}}=a+b\ln\frac{100-[\text{salt}]_{\text{bot}}}{[\text{salt}]_{\text{bot}}} \tag{13}$$

where a and b are adjustable parameters which are evaluated from the intercept and slope of the plotted linear relationships. Consequently, the values of adjustable parameters as a function of molecular weight of PEG are reported in Table 8. Taking into account the reported correlation coefficient values in

Table 5. Weight Fraction Percentage (wt %) Obtained by DOE for the Coexisting Phases of $[C_4mim]CH_3COO(1)+K_2HPO_4$ (2)+H_2O+PEG 2000 Along with Their Respective Values of STL and TLL*

		Feed		Top phase		Bottom phase				
PEG 2000	Std. order	w_1	w_2	w_1	w_2	w_1	w_2	α	STL	TLL
0	1	10	30	18.833	18.387	3.334	38.765	0.430	−0.761	25.603
	3	10	35	29.386	10.266	1.139	46.306	0.314	−0.784	45.791
	2	15	30	31.389	9.078	0.847	48.068	0.463	−0.783	49.529
	4	15	35	38.576	5.672	0.315	53.267	0.384	−0.804	61.067
	13	12.5	32.5	30.389	9.657	0.981	47.209	0.392	−0.783	47.698
4	9	10	32.5	23.833	13.448	1.464	44.257	0.382	−0.726	38.073
	10	15	32.5	35.679	6.030	0.432	51.147	0.413	−0.781	57.253
	11	12.5	30	25.929	11.825	1.257	45.216	0.456	−0.739	41.517
	12	12.5	35	34.048	6.805	0.468	50.743	0.358	−0.764	55.300
	15	12.5	32.5	29.942	9.093	0.746	48.274	0.403	−0.745	48.862
8	5	10	30	19.870	15.990	1.836	41.588	0.453	−0.705	31.312
	7	10	35	28.714	8.868	0.594	48.135	0.335	−0.716	48.298
	6	15	30	30.879	7.511	0.348	50.751	0.480	−0.706	52.933
	8	15	35	36.974	4.499	0.111	55.667	0.404	−0.720	63.064
	14	12.5	32.5	29.332	8.464	0.431	49.734	0.418	−0.700	50.383

*Standard uncertainties u are $u(w)=0.0001$ and $u(T)=1$ K.

Table 6. Weight Fraction Percentage (wt %) Obtained by DOE for the Coexisting Phases of $[C_4mim]CH_3COO(1)+K_2HPO_4$ (2)+H_2O+PEG 4000 Along with Their Respective Values of STL and TLL*

		Feed		Top phase		Bottom phase				
PEG 4000	Std. order	w_1	w_2	w_1	w_2	w_1	w_2	α	STL	TLL
0	1	10	30	18.610	18.591	3.273	38.913	0.439	−0.755	25.459
	3	10	35	29.018	10.496	1.112	46.452	0.319	−0.776	45.514
	2	15	30	31.559	8.982	0.866	47.940	0.461	−0.788	49.597
	4	15	35	38.860	5.562	0.326	53.104	0.381	−0.811	61.197
	13	12.5	32.5	29.949	9.921	0.940	47.459	0.399	−0.773	47.441
4	9	10	32.5	22.349	13.305	0.426	47.381	0.437	−0.643	40.518
	10	15	32.5	34.383	4.978	0.089	53.672	0.435	−0.704	59.559
	11	12.5	30	26.166	10.155	0.410	0.469	0.469	−0.689	45.412
	12	12.5	35	32.764	5.810	0.112	52.845	0.379	−0.694	57.258
	15	12.5	32.5	29.774	7.590	0.220	50.208	0.416	−0.693	51.863
8	5	10	30	20.893	13.074	0.586	44.629	0.464	−0.644	37.525
	7	10	35	28.533	7.013	0.173	49.839	0.347	−0.662	51.365
	6	15	30	30.511	5.801	0.067	53.297	0.491	−0.641	56.416
	8	15	35	35.939	3.231	0.017	57.733	0.417	−0.659	65.276
	14	12.5	32.5	29.030	6.694	0.101	51.857	0.429	−0.641	53.633

*Standard uncertainties u are $u(w)=0.0001$ and $u(T)=1$ K.

Table 7. Weight Fraction Percentage (wt %) Obtained by DOE for the Coexisting Phases of $[C_4mim]CH_3COO(1)+K_2HPO_4$ (2)+H_2O+PEG 6000 Along with Their Respective Values of STL and TLL*

		Feed		Top phase		Bottom phase				
PEG 6000	Std. order	w_1	w_2	w_1	w_2	w_1	w_2	α	STL	TLL
0	1	10	30	18.908	18.318	3.354	38.716	0.427	−0.763	25.652
	3	10	35	28.949	10.539	1.107	46.479	0.319	−0.775	45.463
	2	15	30	31.209	9.180	0.827	48.205	0.467	−0.779	49.457
	4	15	35	38.946	5.529	0.330	53.055	0.380	−0.813	61.237
	13	12.5	32.5	30.071	9.847	0.951	47.389	0.397	−0.776	47.512
4	9	10	32.5	22.287	11.475	0.052	49.522	0.447	−0.584	44.068
	10	15	32.5	33.784	3.844	0.006	55.374	0.444	−0.655	61.615
	11	12.5	30	26.055	8.486	0.048	49.764	0.479	−0.630	48.787
	12	12.5	35	32.293	4.563	0.009	54.207	0.387	−0.650	59.218
	15	12.5	32.5	29.231	6.306	0.022	52.036	0.427	−0.639	54.262
8	5	10	30	20.850	10.075	0.317	47.783	0.472	−0.545	42.936
	7	10	35	28.042	4.763	0.130	51.541	0.354	−0.597	54.473
	6	15	30	29.970	3.778	0.036	56.212	0.500	−0.571	60.377
	8	15	35	35.211	1.838	0.013	59.591	0.426	−0.609	67.634
	14	12.5	32.5	28.611	4.455	0.065	54.145	0.436	−0.574	57.306

*Standard uncertainties u are $u(w)=0.0001$ and $u(T)=1$ K.

Table 8, it is reasonable to conclude that this correlation is adequate for the assessment of the TL data.

Effect of PEG on tie-lines

The effect of PEG concentration and its molecular weight as an additive on the TLLs and STLs is illustrated in Figure 5. This figure is plotted at the center points of initial concentration of $[C_4mim]CH_3COO$ and K_2HPO_4.

Table 8. Parameters of Othmer–Tobias Equations Along with Their Correlation Coefficients (R^2)

	PEG	Othmer–Tobias		
Biphasic System	wt %	a	b	R^2
$[C_4mim]CH_3COO+K_2HPO_4$	0	0.743	1.563	0.923
+PEG 2000	4	0.745	1.137	0.793
	8	0.678	2.047	0.982
$[C_4mim]CH_3COO+K_2HPO_4$	0	0.655	1.788	0.996
+PEG 4000	4	0.927	1.987	0.905
	8	0.991	1.386	0.969
$[C_4mim]CH_3COO+K_2HPO_4$	0	0.661	1.728	0.999
+PEG 6000	4	1.103	2.122	0.906
	8	1.144	1.383	0.924

It is obvious that an increase in PEG concentration leads to a rise in STLs and TLLs values. In these systems, the absolute values of slope of tie-lines climb in the following order: 8 wt % of PEG< 4 wt % of PEG< No PEG. Thus, it is reasonable to conclude that with decrease in polymer concentration, water is driven from top phase to bottom phase. Additionally, the augmentation of the molecular weight of PEG induced a slight increase in TLLs and STLs.

Partitioning of the PEG in IL-ATPS

Physical and chemical nature of PEG as an additive affects its subsequent partitioning between the two phases. Hence, evaluation of the partitioning behavior of PEG in IL-based ATPS is crucial to comprehend its impact on extraction ability of ATPS. The partitioning coefficient of PEG is defined in the same manner, thus, it is known to be the ratio of PEG concentration in IL-rich phase to that in K_2HPO_4-rich phase

$$K_{PEG}=\frac{[PEG]_{IL}}{[PEG]_{salt}} \tag{14}$$

where $[PEG]_{IL}$ and $[PEG]_{salt}$ are the concentrations of PEG in IL and inorganic salt aqueous phase, respectively. Figure 6

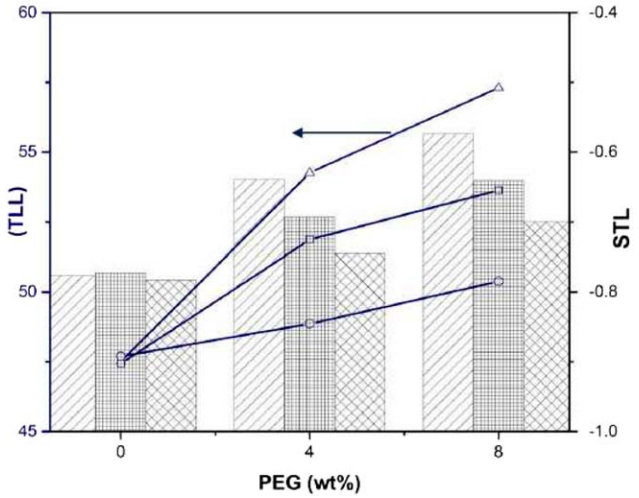

Figure 5. Effect of PEG on TLLs and STLs in center point of $[C_4mim]CH_3COO$ and K_2HPO_4 initial concentration in DOE table.

TLL: -△-, PEG 6000; -□-, PEG 4000; and -○-, PEG 2000. STL: ▨, PEG 6000; ▤, PEG 4000; and ▧, PEG 2000. [Color figure can be viewed in the online issue, which is available at wileyonlinelibrary.com.]

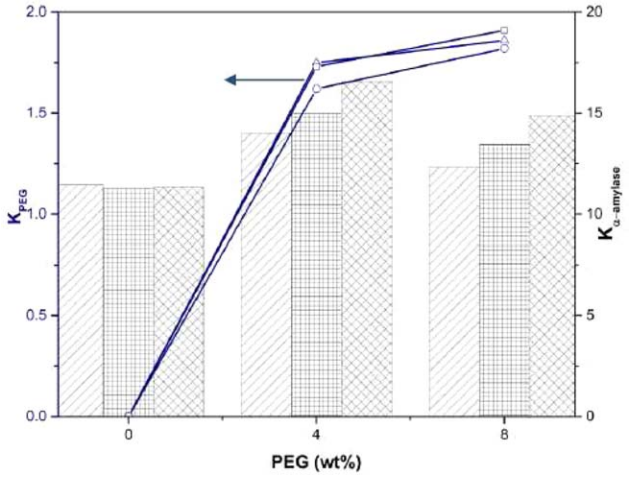

Figure 6. Effect of PEG on and K_{PEG} and $K_{\alpha\text{-amylase}}$ in center point of $[C_4mim]CH_3COO$ and K_2HPO_4 initial concentration in DOE table.

K_{PEG}: -△-, PEG 6000; -□-, PEG 4000; and -○-, PEG 2000. $K_{\alpha\text{-amylase}}$: ▨, PEG 6000; ▤, PEG 4000; and ▧, PEG 2000. [Color figure can be viewed in the online issue, which is available at wileyonlinelibrary.com.]

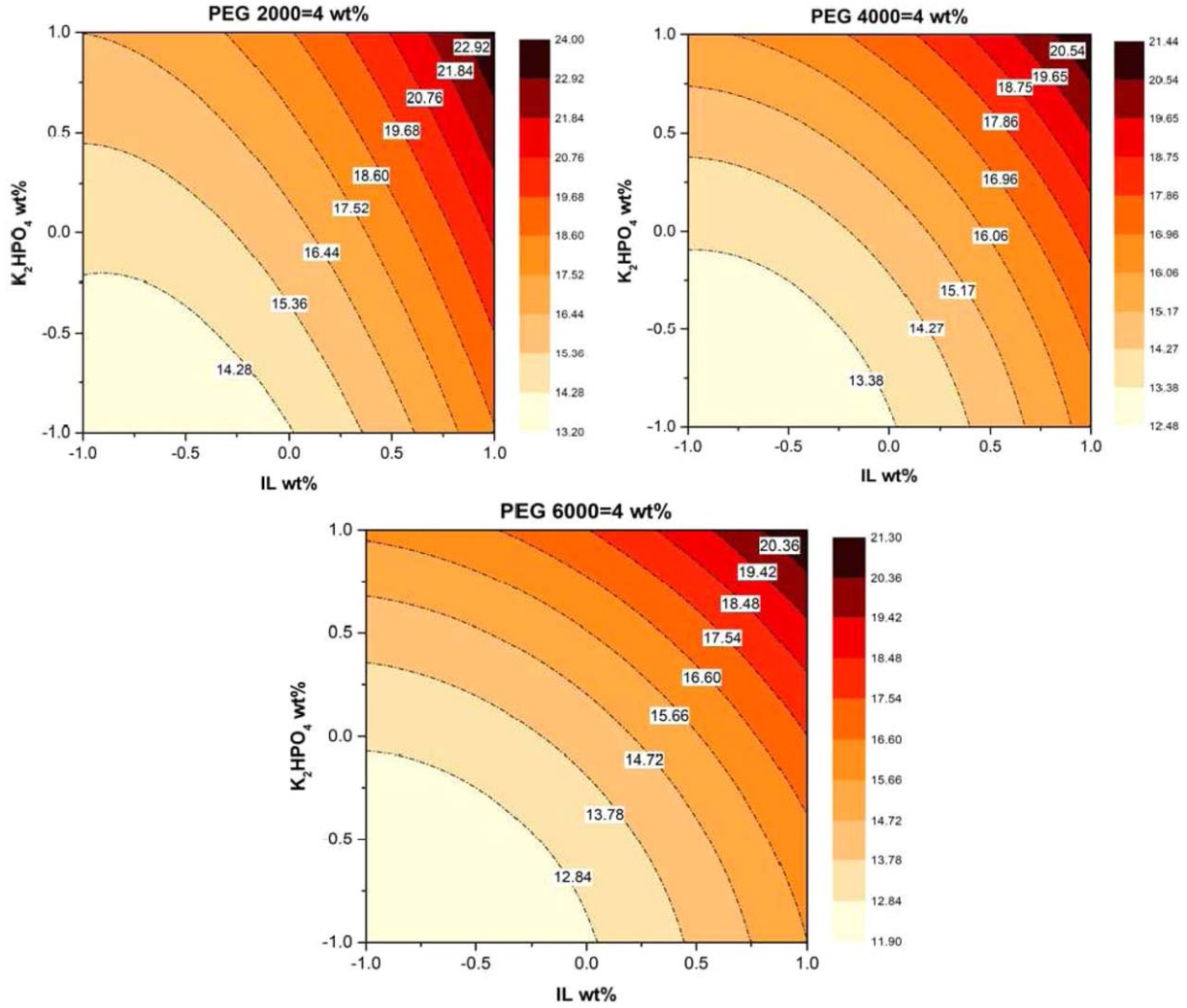

Figure 7. Contour plots of effects of initial concentrations of $[C_4mim]CH_3COO$ and K_2HPO_4 on partitioning coefficient of α-amylase (a) PEG 2000 (b) PEG 4000, and (c) PEG 6000.

[Color figure can be viewed in the online issue, which is available at wileyonlinelibrary.com.]

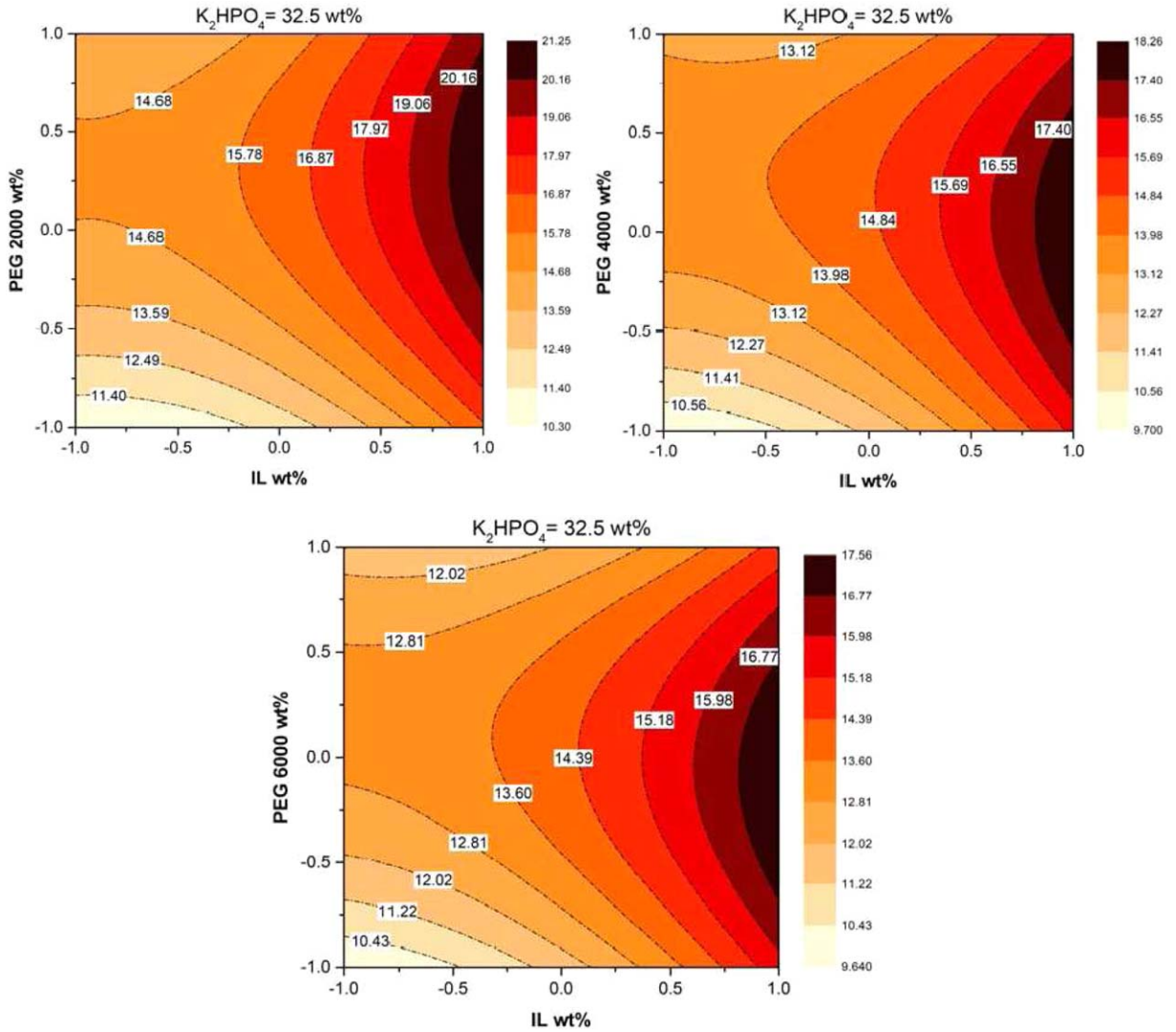

Figure 8. Contour plots of effects of initial concentrations of [C_4mim]CH_3COO and PEG on partitioning coefficient of α-amylase (a) PEG 2000 (b) PEG 4000, and (c) PEG 6000.

[Color figure can be viewed in the online issue, which is available at wileyonlinelibrary.com.]

represents the partitioning coefficients of PEG as the function of its molecular weight and concentrations at the center points of [C_4mim]CH_3COO and K_2HPO_4 concentrations. The PEG in all cases partitioned preferentially to IL-rich phase. The partitioning behavior of PEG is related to its hydrophobicity/hydrophilicity. PEG with lower molecular weight is more hydrophilic and migrates to the inorganic-rich phase. Presence of PEG in each phase defines its physical and chemical properties; thus, enhancement in α-amylase partitioning is observed by presence of PEG.

Table 9. ANOVA Table for the Partition Coefficient of α-Amylase in [C_4mim]CH_3COO+K_2HPO_4+water+PEG 2000 ATPS

Source	Sum of squares	DF	Mean square	*F*-value	*P*-value
Model	200.25	7	28.61	43.98	<0.0001
IL	101.39	1	101.39	155.89	<0.0001
Salt	46.22	1	46.22	71.06	<0.0001
PEG	26.50	1	26.50	40.74	0.0004
IL×salt	2.69	1	2.69	4.14	0.0813
Salt×PEG	2.72	1	2.72	4.18	0.0801
IL^2	8.04	1	8.04	12.36	0.0098
PEG^2	19.34	1	19.34	29.74	0.0010
Residual	4.55	7	0.65		
Total	204.80	14			

Effect of process variables

Effect of Feed's Initial Concentration. In this study, different initial concentration of [C_4mim]CH_3COO, $K_2HPO_4$and

Table 10. ANOVA Table for the Partition Coefficient of α-Amylase in [C_4mim]CH_3COO+K_2HPO_4+ water+PEG 4000 ATPS

Source	Sum of squares	DF	Mean square	*F*-value	*P*-value
Model	128.53	9	14.28	30.11	0.0008
IL	55.74	1	55.74	117.52	0.0001
Salt	43.73	1	43.73	92.20	0.0002
PEG	7.10	1	7.10	14.98	0.0118
IL×salt	1.24	1	1.24	2.61	0.1669
IL×PEG	4.31	1	4.31	9.09	0.0296
Salt×PEG	2.28	1	2.28	4.80	0.0799
IL^2	3.70	1	3.70	7.80	0.0383
$Salt^2$	1.27	1	1.27	2.68	0. 1623
PEG^2	12.99	1	12.99	27.38	0.0034
Residual	2.37	5	0.47		
Total	130.90	14			

Table 11. ANOVA Table for the Partition Coefficient of α-Amylase in [C_4mim]CH_3COO+K_2HPO_4+water+PEG 6000 ATPS

Source	Sum of squares	DF	Mean square	*F*-value	*P*-value
Model	134.42	9	14.94	20.48	0.0020
IL	52.08	1	52.08	71.42	0.0004
Salt	56.72	1	56.72	77.78	0.0003
PEG	0.56	1	0.56	0.77	0.4196
IL×salt	1.48	1	1.48	2.03	0.2136
IL×PEG	4.25	1	4.25	5.83	0.0605
Salt×PEG	4.03	1	4.03	5.53	0.0655
IL^2	2.83	1	2.83	3.88	0.1058
$Salt^2$	2.24	1	2.24	3.07	0.1401
PEG^2	14.33	1	14.33	19.65	0.0068
Residual	3.65	5	0.73		
Total	138.06	14			

PEG were investigated to evaluate their effects on biomolecule's partitioning. Table 2 presents the complete design matrix with their subsequent response values. Response contour plots of 7a, 7b, and 7c (Figure 7) are the visual indications of the fact that an increase in the initial concentration of [C_4mim] CH_3COO and K_2HPO_4 leads to a rise in α-amylase partitioning. An increase in the initial concentration of inorganic salt makes the space of the bottom phase more packed and thus, α-amylase preferentially migrates to the top phase.

In IL-based ATPSs, the IL-rich and inorganic salt-rich phases are of distinct nature. The presence of high charge density species in K_2HPO_4 –rich phase make it more hydrophilic while [C_4mim]CH_3COO-rich aqueous phase is mainly hydrophobic in nature.[39] Hence, the variation in the phases polarities is the governing factor affecting $K_{\alpha\text{-amylase}}$. The capability of ionic liquids' anions to form the hydrogen bond between the solute and the solvent determines its hydrophobicity. The reported hydrogen bond basicity (β) for [C_4mim]CH_3COO is 1.2.[40] Consequently, an increase in the initial concentration of [C_4mim]CH_3COO makes the IL-rich phase more hydrophobic and therefore an augmentation in the partitioning coefficient is observed. Thus, it can be stated that the extraction process is mainly controlled by the hydrophobic interactions.

The effect of additive's initial concentration in the feed for PEG 2000, 4000, and 6000 are shown in Figures 8a–c. With an increase in PEG weight percent, the partitioning coefficient increases while a slight decrease is observed at high PEG concentrations. This effect can be due to the interactions among α-amylase and PEG molecules. PEG molecules may exclude α-amylase molecules to lower phase at high polymer concentration. However, at low concentrations of PEG this effect is less pronounced.

Effect of Polymer Molecular Weight. The experimental data (Figure 6) indicated that $K_{\alpha\text{-amylase}}$ decreases with an increase in PEG molecular weight, which is in accordance with the observations of Zhi et al.[41] and Schmid et al.[42] With an increase in the molecular weight of PEG, the number of hydroxyl groups for the same concentration of PEG decreases. Consequently, the hydrophobicity of the upper phase improves. Additionally, less space is available for the partitioning of the biomolecule in the upper phase. Hydrophobic interaction chromatography evaluated a relatively high surface hydrophobicity for α-amylase;[42] thus, the size-exclusion effect is suggested to be the main reason for the decrease in the partitioning coefficients.

Development of regression model equation

For evaluation of α-amylase's partitioning coefficient a second-order polynomial regression equation was developed. The represented equations evaluate the effect of independent process variables on the response. Furthermore, confidence level of 95% was appointed in the analysis of response surface which means that the effects with less than 95% significance were not considered. Regression models in the coded values are represented as follows

IL+ K_2HPO_4+PEG 2000

$$K_{\alpha\text{-amylase}} = 16.90 + 3.18x_1 + 2.15x_2 + 1.63x_3 + 0.58x_1x_2 + 1.69x_1^2 - 2.63x_3^2 \quad (15)$$
$$R^2 = 0.9778$$

IL+ K_2HPO_4+PEG 4000

$$K_{\alpha\text{-amylase}} = 14.69 + 2.36x_1 + 2.09x_2 + 0.84x_3 + 0.39x_1x_2 - 0.73x_1x_3 + 0.53x_2x_3 + 1.2x_1^2 + 0.70x_2^2 - 2.25x_3^2 \quad (16)$$
$$R^2 = 0.9819$$

IL+ K_2HPO_4+PEG 6000

$$K_{\alpha\text{-amylase}} = 14.20 + 2.28x_1 + 2.38x_2 + 0.24x_3 + 0.43x_1x_2 - 0.73x_1x_3 + 0.71x_2x_3 + 1.05x_1^2 + 0.93x_2^2 - 2.36x_3^2 \quad (17)$$
$$R^2 = 0.9736$$

Each regression equation has a unique R^2-value, which is a mere indication of the adequacy of the model. The R^2-value for Eqs. 15–17 was 0.9778, 0.9819, and 0.9736, respectively. As a result, e.g. 97.78% of total variation in α-amylase partitioning in IL+ K_2HPO_4+PEG 2000 ATPS can be assigned to the experimental variables under investigation. Moreover, all the regression equations had R^2-values which were close to unity which indicated the agreement between experimental and predicted *K*-value.

The statistical significance of the regression model was assessed by the analysis of variance (ANOVA). Table 9–11 tabulate the *F*-test and *P*-values for the significant linear, quadratic and interaction effects. Thus, taking into account the ANOVA analysis for all three systems, the significance of models are validated.

The optimization of the response was performed to obtain the optimum values of the process variables (Table 12). These data are in close agreement with those obtained from RSM, indicating that RSM is a good statistical method to optimize the process parameters in complex processes.

Table 12. Optimum Operating Conditions of the Process Variables for Maximum Partition Coefficient at *T*=298.15 K

	Optimum level			$K_{\alpha\text{-amylase}}$	
Biphasic system	IL wt %	Salt wt %	PEG wt %	Predicted	Experimental
[C_4mim]CH_3COO+K_2HPO_4+PEG 2000	14.97	34.76	4.65	23.63	24.12
[C_4mim]CH_3COO+K_2HPO_4+PEG 4000	14.68	34.66	5.78	20.12	21.27
[C_4mim]CH_3COO+K_2HPO_4+PEG 6000	14.04	34.91	4.56	19.43	19.18

Optimization procedure

The purpose of optimization is the evaluation of a combination of factor levels that can satisfy the desired requirements for responses and factors. The alternative goals are either maximize, minimize, target, within range, or an exact value. Hence, a desired goal is appointed to each independent variable and response and an overall desirability function is resulted by the combination of the goals. Two or more optimum values can be estimated from the optimization procedure due to the curvature of the response surface.

In our optimization studies, we tried to maximize the partition coefficient of α-amylase with goal selection to be within range for three independent variables. Table 12 demonstrates the optimization results. Some experimental runs were conducted to evaluate the efficiency of the models; the experimental results are tabulated in Table 12. It can be observed that the experimental results are congruent with the predicted partition coefficient.

Conclusion

The application of PEGs as additive in $[C_4mim]CH_3COO$-based ATPS for enhancement of extraction of α-amylase was studied. The quaternary phase diagrams of $[C_4mim]$-CH_3COO+ K_2HPO_4+ 4/8 wt % PEG (2000, 4000, and 6000)+ water was established and it was compared with ternary phase diagram of $[C_4mim]CH_3COO$+ K_2HPO_4+ water. A three- parameter equation was employed in order to correlate the binodal data. The presence of PEG as additive with higher molecular weight and concentration expanded the two phase area. Furthermore, the concentration effect of phase forming components on partition coefficient of α-amylase was studied by the use of RSM based on three-variable CCD. The regression models along with the ANOVA successfully estimated the effect of process variables on extraction. Moreover, foe each experimental run the TLs were evaluated and validated with a proper model. It was observed that PEGs would preferentially migrate to IL-rich phase and thus it noticeably increased the partition coefficients. The optimization studies were carried out and the subsequent results were reported. To sum up, addition of PEG as adjuvants in IL-based ATPS enhanced the partition coefficients of biomolecule and with proper selection of process variables $K_{\alpha\text{-amylase}}$ could be optimized.

Literature Cited

1. Hatti-Kaul R. *Aqueous Two-Phase Systems: Methods and Protocols*. New Jersey: Humana Press, 2000.
2. Saravanan S, Rao JR, Nair BU, Ramasami T. Aqueous two-phase poly(ethylene glycol)–poly(acrylic acid) system for protein partitioning: Influence of molecular weight, pH and temperature. *Process Biochem*. 2008;43:905–911.
3. Oshima T, Suetsugu A, Baba Y. Extraction and separation of a lysine-rich protein by formation of supramolecule between crown ether and protein in aqueous two-phase system. *Anal Chim Acta*. 2010;674:211–219.
4. Yu C, Han J, Wang Y, Yan Y, Hu S, Li Y, Zhao X. Liquid–liquid equilibrium composed of imidazolium tetrafluoroborate ionic liquids + sodium carbonate aqueous two-phase systems and correlation at (288.15, 298.15, and 308.15) K. *Thermochim Acta*. 2011;523:221–226.
5. Akama Y, Sali A. Extraction mechanism of Cr(VI) on the aqueous two-phase system of tetrabutylammonium bromide and $(NH4)_2SO_4$ mixture. *Talanta*. 2002;57:681–686.
6. Martiak J, Schlosser S. Extraction of lactic acid by phosphonium ionic liquids. *Sep Purif Technol*. 2007;57:483–494.
7. Bora M, Borthakur S, Rao PC, Dutta NN. Aqueous two-phase partitioning of cephalosporin antibiotics: effect of solute chemical nature. *Sep Purif Technol*. 2005;45:153–156.
8. Jiang YY, Xia HS, Yu J, Guo C, Liu HZ. Hydrophobic ionic liquids-assisted polymer recovery during penicillin extraction in aqueous two-phase system. *Chem Eng J*. 2009;147:22–26.
9. Mokhtarani B, Karimzadeh R, Amini MH, Manesh SD. Partitioning of ciprofloxacin in aqueous two-phase system of poly(ethylene glycol) and sodium sulphate. *Biochem Eng J*. 2008;38:241–247.
10. Albertsson, PA. *Partitioning of Cell Particles and Macromolecules*, 3rd ed. New York: Wiley, 1986.
11. Madeira PP, Reis CA, Rodrigues AE, Mikheeva LM, Zaslavsky BY. Solvent properties governing solute partitioning in polymer/polymer aqueous two-phase systems: nonionic compounds. *J Phys Chem B*. 2010;114:457−462.
12. Shahriari S, Neves CMSS, Freire MG, Coutinho JAP. Role of the Hofmeister series in the formation of ionic liquid-based aqueous biphasic systems. *J Phys Chem B*. 2012;116:7252–7258.
13. Abdolrahimi S, Nasernejad B, Pazuki G. Prediction of partition coefficients of alkaloids in ionic liquids based aqueous biphasic systems using hybrid group method of data handling (GMDH) neural network. *J Mol Liq*. 2014;191:79–84.
14. Freire MG, Filipa A, Claudio M. Aqueous biphasic systems: a boost brought about by using ionic liquids. *Chem Soc Rev*. 2012;41:4966–4995.
15. Pereira JF, Lima AS, Freire MG, Coutinho JAP. Ionic liquids as adjuvants for the tailored extraction of biomolecules in aqueous biphasic systems. *Green Chem*. 2010;12:1661–1669.
16. Raja S, Murty VR, Thivaharan V, Rajasekar V, Ramesh V. Aqueous two phase systems for the recovery of biomolecules—a review. *Sci Technol*. 2011;1:7–16.
17. Almeida MR, Passos H, Pereira MM, Lima AS, Coutinho JAP, Freire MG. Ionic liquids as additives to enhance the extraction of antioxidants in aqueous two-phase systems. *Sep Purif Technol*. 2014; 128:1–10.
18. Gutowski KE, Broker GA, Willauer HD, Huddleston JG, Swatloski RP, Holbrey JD, Rogers RD. Controlling the aqueous miscibility of ionic liquids: aqueous biphasic systems of water-miscible ionic liquids and water-structuring salts for recycle, metathesis, and separations. *J Am Chem Soc*. 2003;125:6632–6633.
19. Ventura SPM, Sousa SG, Serafim LS, Lima AS, Freire MG, Coutinho JAP. Ionic liquids based aqueous two-phase systems with ph controlled by phosphate buffer: the anion effect. *J Chem Eng Data*. 2012;57:507–512.
20. Ventura SPM, Sousa SG, Serafim LS, Lima AS, Freire MG, Coutinho JAP. Ionic liquid based aqueous biphasic systems with controlled pH: the ionic liquid cation effect. *J Chem Eng Data*. 2011;56:4253–4260.
21. Dreyer S, Kragl U. Ionic liquids for aqueous two-phase extraction and stabilization of enzymes. *Biotechnol Bioeng*. 2008;99:1416–1424.
22. Freire MG, Louros CLS, Rebelo LPN, Coutinho JAP. Aqueous biphasic systems composed of a water-stable ionic liquid + carbohydrates and their applications. *Green Chem*. 2011;13:1536–1545.
23. Han J, Wang Y, Li YF, Yu CL, Yan YS. Equilibrium phase behavior of aqueous two phase systems containing 1-alkyl-3-methylimidazolium tetrafluoroborate and ammonium tartrate at different temperatures: experimental determination and correlation. *J Chem Eng Data*. 2011; 56:3679–3687.
24. Domınguez-Perez M, Tome LIN, Freire MG, Marrucho IM, Cabeza O, Coutinho JAP. (Extraction of biomolecules using) aqueous biphasic systems formed by ionic liquids and aminoacids. *Sep Purif Technol*. 2010;72:85–91.
25. Rosa PAJ, Azevedo AM, Ferreira IF, Vries J, Korporaal R, Verhoef HJ, Visser TJ, Aires-Barros MR. Affinity partitioning of human antibodies in aqueous two-phase systems. *J Chromatogr A*. 2007;1162: 103–113.
26. Passos H, Ferreira AR, Filipa A, Cláudio M. Characterization of aqueous biphasic systems composed of ionic liquids and a citrate-based biodegradable salts. *Biochem Eng J*. 2012;67:68–76.
27. Visser AE, Swatloski RP, Reichert WM, Mayton R, Sheff S, Wierzbicki A, Davis JH, Rogers RD. Task-specific ionic liquids incorporating novel cations for the coordination and extraction of Hg 2+ and Cd 2+: synthesis, characterization, and extraction studies. *Environ Sci Technol*. 2002;36:2523–2529.
28. Davis JH. Ionic Liquids: industrial applications to green chemistry. *ACS Symp Ser*. 2002;818:247–258.

29. Ravikumar K, Ramalingam S, Krishnan S, Balu K. Application of response surface methodology to optimize the process variables for Reactive Red and Acid Brown dye removal using a novel adsorbent. *Dyes Pigm.* 2006;70:18–26.
30. Box G, Draper N. *Empirical Model Building and Response Surfaces*. Wiley, 1987.
31. Merchuk JC, Andrews BA, Asenjo JA. Aqueous two-phase systems for protein separation. Studies on phase inversion. *J Chromatogr B*. 1998;711:285–293.
32. Myers RH, Montgomery DC. *Response Surface Methodology: Process and Product Optimization Using Designed Experiments*, 2nd ed. Wiley, 2002.
33. Montgomery DC. *Design and Analysis of Experiments*, 4th ed. Wiley, 1996.
34. Guan Y, Lilley T, Treffry TH. A new excluded volume theory and its application to the coexistence curves of aqueous polymer two-phase systems. *Macromolecules*. 1993;26:3971−3979.
35. Han J, Wang Y, Yu C, Li Y, Kang W, Yan Y. (Liquid + liquid) equilibrium of (imidazolium ionic liquids + organic salts) aqueous two-phase systems at T = 298.15 K and the influence of salts and ionic liquids on the phase separation. *J Chem Thermodyn*. 2012;45: 59–67.
36. Xie XQ, Han J, Wang Y, Yan YS, Yin GW, Guan WX. Measurement and correlation of the phase diagram data for PPG400 + (K3PO4, K2CO3, and K2HPO4) + H2O aqueous two-phase systems at T = 298.15 K. *J Chem Eng Data*. 2010;55:4741–4745.
37. Huddleston JG, Willauer HD, Rogers RD. Phase diagram data for several PEG + salt aqueous biphasic systems at 25°C. *J Chem Eng Data*. 2003;48:1230–1236.
38. Tubio G, Pellegrini L, Nerli BB, Pico GA.Liquid-liquid equilibria of aqueous two-phase systems containing poly(ethylene glycols) of different molecular weight and sodium citrate. *J Chem Eng Data*. 2006;51:209–212.
39. Abdolrahimi S, Nasernejad B, Pazuki G. Influence of process variables on extraction of Cefalexin in a novel biocompatible ionic liquid based-aqueous two phase system. *Phys Chem Chem Phys*. 2015;17: 655–669.
40. Filipa A, Claudio M, Ferreira AM, Shahriari S, Freire MG, Coutinho JAP. Critical assessment of the formation of ionic-liquid-based aqueous two-phase systems in acidic media. *J Phys Chem B*. 2011;115: 11145–11153.
41. Zhi W, Song J, Bi J, Ouyang F. Partial purification of α-amylase from culture supernatant of Bacillus subtilis in aqueous two-phase systems. *Bioprocess Biosyst Eng*. 2004;27:3–7.
42. Schmid AS, Ventom AM, Asenjo JA. Partitioning and purification of a-amylase in aqueous two-phase systems. *Enzyme Microb Tech*. 1994;16:131–142.

Manuscript received Mar. 12, 2015, and revision received May 31, 2015.